Materials and Methods

Mudstones of an outcrop situated near the village of Alstätte, northwest Germany were studied (N 52°09'04.4'', E 6°54'37.7''; paleolatitude ~39°N). The sequence was deposited in the southern part of the Boreal Realm (Fig. DR1). For geological and stratigraphic background see Bottini and Mutterlose (2012) and Lehmann et al. (2012). The sediments were deposited on a passive shelf area about 30 km off from the paleocoastline with an estimated paleowaterdepth of <200 m. The section exposes bio-, litho- and chemostratigraphically well dated clays, laminated mudstones, and marlstones of 16 m thickness (including the FS), covering the early Aptian, allowing for a detailed bed-by-bed collection of material. The succession yields a rich flora of calcareous nannofossils, allowing the recognition of four biozones (Bottini and Mutterlose, 2012). In Alstätte 1, the $\delta^{13}C_{org}$ curve is relatively noisy and only segments C3, C4-C6 (single segments can not be detected) and C7 could be identified. This is perhaps due to diagenetic effects related to sulphate reduction, as it has also been attested in other sections in the LSB (e.g. Heldt et al., 2012; Pauly et al., 2013).

A total of 14 samples were analyzed for TEX_{86} paleothermometry. For stable isotope analysis ($\delta^{18}O$, $\delta^{13}C$) the low magnesium calcite of 17 belemnites guards were studied. Settling slides for the analyses of calcareous nannofossils have been made following Geisen et al. (1999). For a detailed description of the methodology see Bottini and Mutterlose (2012). The analytical approach for obtaining the stable isotope and trace element composition of the belemnites as well as the organic biomarkers has been described by Mutterlose et al. (2012). The following equation was used for the conversion of TEX_{86} values into SSTs (Kim et al., 2010): $SST = 38.6 + 68.4 * \log (TEX_{86})$.

For the calculation of the TI, we modified the formulas by Tiraboschi et al. (2009) excluding taxa that are sparse and rare in the studied sections (1.1).

The software *"Statsoft Statistica 6"* was used for multivariate "factor analysis" (FA) (R-mode) varimax rotation with principal component extraction to determine the relationships between samples and variables, and to identify/support paleoceanographic and paleoecological affinities among selected nannofossil taxa (Fig. DR2).

(1.1) $TI = (Ss + Ef + Rp) / (Ss + Ef + Rp + Ra + Zd) \times 100$

Where: *Ss =S.stradneri; Ef=E.floralis; Rp=R.parvidentatum; Ra=R.asper; Zd=Z.diplogrammus*.

For each studied site (Alstätte 1 and A39) two significant factors were extracted from the FA (R-mode) varimax rotation analysis:

In Alstätte (Figure DR2A) Factor 2 (F2) and Factor 3 (F3) represent 24% of the total variance. F2 (14% of the total variance) shows positive loadings for*, Z. diplogrammus, C. hayi, R. asper, B. constans, Z. erectus, D. rotatorius*, and negative loadings for *W. barnesiae, S. stradneri, E. floralis, R. parvidentatum*. F3 (11% of the total variance) shows the highest positive loadings for *R. parvidentatum, B. constans, Z. erectus, D. rotatorius* and the highest negative loadings for *W.*

barnesiae, R. asper, Z. diplogrammus. F2 is interpreted to correspond to surface water temperature and F3 to surface water fertility, respectively.

In A39 (Figure DR2B) Factor 1 (F1) and Factor 2 (F2) represent 54% of the total variance. F1 (31% of the total variance) shows the highest positive loadings for *E. floralis, R. parvidentatum, C. hayi,* and the highest negative loadings for *R. asper, W. barnesiae*. F2 (23% of the total variance) shows positive loadings for *D. rotatorius, B. constans, Z. erectus* and negative loadings for *R. asper, W. barnesiae.* F1 is interpreted to correspond to surface water temperature and F2 to surface water fertility, respectively.

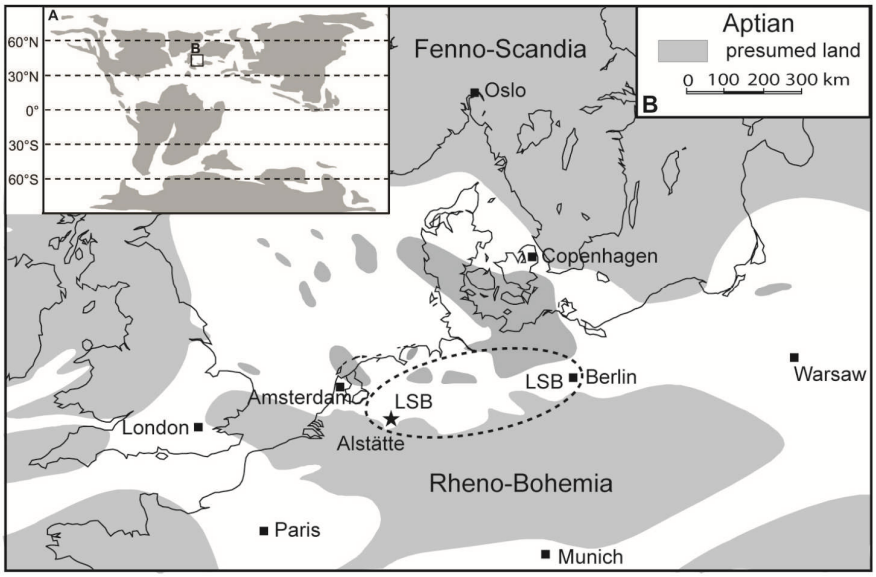

Figure DR1 (A) Paleogeographical map of the early Aptian (~126 Ma). (B) Detailed map showing the studied site. Abbreviations: LSB= Lower Saxony Basin. Maps (A) modified after Smith et al. (1996) and (B) after Pauly et al. (2013).

A

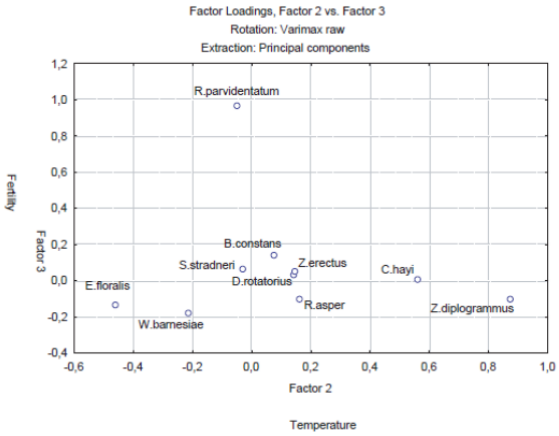

Factor Loadings (Varimax raw) Extraction: Principal components			
	Factor - 1	**Factor - 2**	**Factor - 3**
W. Barnesiae	0.71	0.21	0.17
R. asper	0.87	0.16	-0.10
B. constans	0.92	0.07	0.15
D. rotatorius	0.82	0.14	0.04
Z. erectus	0.94	0.15	0.05
E. floralis	0.52	-0.46	-0.13
R. parvidentatum	0.07	-0.05	0.97
C. hayi	0.77	0.56	0.01
Z. diplogrammus	0.19	0.87	-0.10
S. stradneri	0.91	-0.03	0.07
Expl.Var	5.40	1.40	1.00
Prp.Totl	0.54	0.14	0.10

B

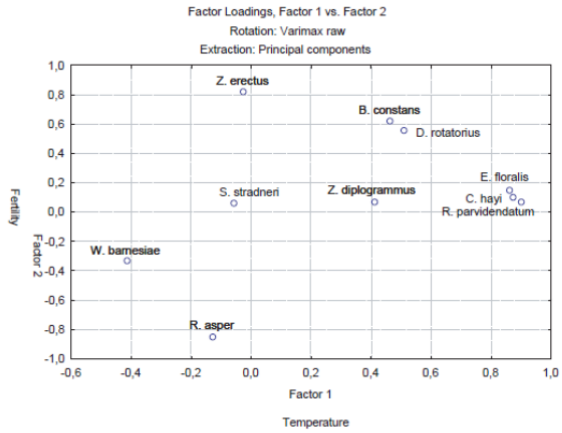

Factor Loadings (Varimax raw) Extraction: Principal components			
	Factor - 1	**Factor - 2**	**Factor - 3**
B. constans	0.46	0.63	0.07
C. hayi	0.87	0.10	0.18
D. rotatorius	0.51	0.56	-0.04
R. parvidendatum	0.90	0.07	0.04
R. asper	-0.13	-0.84	-0.10
S. stradneri	-0.06	0.06	0.87
W. barnesiae	-0.42	-0.33	-0.60
Z. diplogrammus	0.41	0.08	0.54
Z. erectus	-0.03	0.83	0.13
E. floralis	0.86	0.16	-0.01
Expl.Var	3.10	2.20	1.40
Prp.Totl	0.31	0.23	0.15

Figure DR2. Results of Factor Analysis (R-mode) varimax normalized rotation with principal component extraction are presented for (A) Alstätte 1, (B) A39.

Table DR1. TEX86 data from the Barremian-Aptian of the Lower Saxony Basin (Alstätte 1, A 39 sections; paleolatitude ~39°N).

Alstätte 1 section

Substage	Nannofossil zone	m above base	TEX86	BIT	T [°C] SST
Lower Aptian	*N. truittii*	12.8	0.76	0.15	30.3
Lower Aptian	*E. floralis*	10.3	0.79	0.11	31.6
Lower Aptian	*E. floralis*	8.8	0.80	0.08	32.1
Lower Aptian	*E. floralis*	7.8	0.80	0.07	32.1
Lower Aptian	*F. oblongus*	6.8	0.83	0.35	33.2
Lower Aptian	*F. oblongus*	6.2	0.81	0.39	32.3
Lower Aptian	*F. oblongus*	5.6	0.79	0.08	31.6
Lower Aptian	*F. oblongus*	5.3	0.82	0.03	32.6
Lower Aptian	*F. oblongus*	4.9	0.80	0.04	31.8
Lower Aptian	*F. oblongus*	3.7	0.82	0.05	32.8
Lower Aptian	*F. oblongus*	3.4	0.78	0.09	31.0
Lower Aptian	*F. oblongus*	3.2	0.71	0.14	28.5
Lower Aptian	*C. litterarius*	1.7	0.73	0.11	29.3
Lower Aptian	*C. litterarius*	0.35	0.68	0.11	27.3

A39 section

Substage	Belemnite zone	m above base	TEX86	BIT	T [°C] SST
Lower Aptian	*N. ewaldi*	94.4	0.87		34.5
Lower Aptian	*N. ewaldi*	94.3	0.86		34.1
Lower Aptian	*N. ewaldi*	94.2	0.86		34.1
Lower Aptian	*N. ewaldi*	94.0	0.85		33.8
Lower Aptian	*N. ewaldi*	91.6	0.79		31.6
Lower Aptian	*N. ewaldi*	91.1	0.83		33.1
Upper Barremian	*O. depressa*	80.9	0.70		28.0
Upper Barremian	*O. depressa*	76.6	0.75		30.1
Upper Barremian	*O. depressa*	75.9	0.73		29.3
Upper Barremian	*O. depressa*	74.6	0.73		29.3
Upper Barremian	*O. depressa*	71.3	0.74		29.7
Upper Barremian	*O. depressa*	66.1	0.70		28.0
Upper Barremian	*O. depressa*	64.5	0.70		28.0
Upper Barremian	*O. depressa*	59.7	0.75		30.1
Upper Barremian	*O. depressa*	50.1	0.66		26.3
Upper Barremian	*O. depressa*	43.7	0.71		28.4
Upper Barremian	*O. depressa*	38.1	0.70		28.0
Upper Barremian	*O. germanica*	37.0	0.71		28.4
Upper Barremian	*O. germanica*	34.0	0.70		28.0
Upper Barremian	*O. germanica*	22.6	0.66		26.3
Upper Barremian	*O. germanica*	21.6	0.68		27.1
Upper Barremian	*O. brunsvicensis*	21.4	0.69		27.6
Upper Barremian	*O. brunsvicensis*	21.2	0.70		28.0
Upper Barremian	*O. brunsvicensis*	18.4	0.70		28.0
Upper Barremian	*O. brunsvicensis*	13.5	0.68		27.1
Lower Barremian	*Aulacoteuthis* spp.	10.0	0.72		28.8
Lower Barremian	*Aulacoteuthis* spp.	8.5	0.65		25.8
Lower Barremian	*Aulacoteuthis* spp.	7.8	0.68		27.1
Lower Barremian	*Aulacoteuthis* spp.	6.5	0.67		26.7
Lower Barremian	*P. pugio*	2.0	0.66		26.3

Table DR2. Stable isotope and trace element data from belemnites of the Alstätte 1 section.

Alstätte 1 section

Substage	Nannofossil zone	m above base	Taxon	$\delta^{13}C$ [‰]	$\delta^{18}O$ [‰]	T°C ($\delta^{18}O_{SW}$ = -1%)	T°C ($\delta^{18}O_{SW}$ = +1%)	Mg [ppm]	Sr [ppm]	Fe [ppm]	Mn [ppm]
Lower Aptian	*N. truittii*	13.7	*N. ewaldi*	4.10	0.01	11.4	20.1	1594	1191	262	18
Lower Aptian	*N. truittii*	13.7	*N. ewaldi*	3.70	-0.25	12.5	21.4	1952	1272	88	27
Lower Aptian	*N. truittii*	13.7	*N. ewaldi*	3.57	-0.22	12.4	21.2	1631	1242	146	57.6
Lower Aptian	*N. truittii*	13.7	*N. ewaldi*	3.83	-0.93	15.4	24.6	1993	1304	227	41.2
Lower Aptian	*N. truittii*	13.7	*N. ewaldi*	3.94	-0.44	13.3	22.2	2029	1085	245	62.3
Lower Aptian	*N. truittii*	13.7	*N. ewaldi*	2.15	-0.79	14.8	23.9	2756	1201	89	8.2
Lower Aptian	*N. truittii*	13.7	*N. ewaldi*	2.48	-0.50	13.5	22.5	1536	1214	175	4.5
Lower Aptian	*E. floralis*	7.5	*Neohibolites* sp.	-0.16	-0.52	13.6	22.6	3040	1231	16	3.3
Lower Aptian	*E. floralis*	7.5	*Neohibolites* sp.	-0.43	-0.61	14.0	23.0	2525	1314	25	5.4
Lower Aptian	*E. floralis*	7.5	*Neohibolites* sp.	0.73	-0.16	12.1	20.9	1815	1180	302	8.5
Lower Aptian	*E. floralis*	7.5	*D. grasiana*	0.29	-0.70	14.4	23.5	2596	1579	98	16
Lower Aptian	*F. oblongus*	5.1	*N. ewaldi*	-1.15	-1.01	15.7	24.9	2877	1427	298	9.4
Lower Aptian	*F. oblongus*	3.5	*O. depressa*	1.89	-0.41	13.2	22.1	1951	1104	17	2.2
Lower Aptian	*F. oblongus*	3.5	*O. depressa*	1.27	-0.62	14.1	23.1	2272	1204	15	4.1
Lower Aptian	*C. litterarius*	1.9	*O. depressa*	3.08	0.07	11.2	19.9	1376	1130	32	1.8
Lower Aptian	*C. litterarius*	0.2	*H. minutus*	0.83	-0.11	11.9	20.7	1408	1238	21	2.1
Lower Aptian	*C. litterarius*	0.2	*O. depressa*	1.30	0.16	10.8	19.4	2269	1187	20	1.7

Table DR3. TEX86 data from the Hauterivian–Aptian of the Lower Saxony Basin (Gott, Moorberg, A 39 and Alstätte 1 sections; paleolatitude ~39°N) and the Speeton section (paleolatitude ~41°N). Missing BIT value =0, no branched GDGTs were detected. The Hauterivian and Barremian data from Mutterlose et al. (2012). The TEX86 based paleotemperatures have been re-calculated by using the Kim et al. (2010) equation.

Gott section

Substage	Belemnite zone	m above base	TEX86	BIT	T [°C] SST
Upper Barremian	*O. depressa*	66.7	0.77		30.8
Upper Barremian	*O. depressa*	66.1	0.73		29.3
Upper Barremian	*O. germanica*	51.8	0.73		29.3
Lower Barremian	*Aulacoteuthis* spp.	26.7	0.71		28.4
Lower Barremian	*Aulacoteuthis* spp.	25.6	0.69		27.6
Lower Barremian	*Aulacoteuthis* spp.	25.1	0.68		27.1
Lower Barremian	*Aulacoteuthis* spp.	24.6	0.68		27.1
Lower Barremian	*Aulacoteuthis* spp.	23.6	0.69		27.6
Lower Barremian	*Aulacoteuthis* spp.	23.1	0.68		27.1
Lower Barremian	*Aulacoteuthis* spp.	22.6	0.73		29.3
Lower Barremian	*Aulacoteuthis* spp.	21.1	0.71		28.4
Lower Barremian	*Aulacoteuthis* spp.	20.6	0.68		27.1
Lower Barremian	*Aulacoteuthis* spp.	20.1	0.68		27.1
Lower Barremian	*P. pugio*	19.7	0.74		29.7

Moorberg section

Substage	Ammonite zone	m above base	TEX86	BIT	T [°C] SST
Lower Barremian	*C. fissicostatum*	83.9	0.69	0.04	27.6
Lower Barremian	*C. fissicostatum*	83.4	0.68	0.06	27.1
Lower Barremian	*C. fissicostatum*	83.0	0.68	0.03	27.1
Lower Barremian	*C. fissicostatum*	82.0	0.69	0.02	27.6
Lower Barremian	*C. fissicostatum*	81.5	0.68	0.03	27.1
Lower Barremian	*C. fissicostatum*	81.0	0.73	0.02	29.3
Lower Barremian	*C. fissicostatum*	79.5	0.71	0.02	28.4
Lower Barremian	*C. fissicostatum*	79.0	0.68	0.03	27.1
Lower Barremian	*C. fissicostatum*	78.5	0.68	0.09	27.1
Lower Barremian	*C. fissicostatum*	78.1	0.74	0.03	29.7
Upper Hauterivian	*S. discofalcatus*	60.0	0.66	0.04	26.3
Upper Hauterivian	*S. gottschei*	55.5	0.63	0.03	24.9
Upper Hauterivian	*S. gottschei*	48.1	0.64	0.03	25.3
Upper Hauterivian	*S. gottschei*	42.2	0.67	0.08	26.7
Upper Hauterivian	*S. gottschei*	39.5	0.66	0.03	26.3
Upper Hauterivian	*Aegocrioceras* spp.	29.0	0.61	0.03	23.9
Lower Hauterivian	*E. regale*	28.0	0.64	0.04	25.3
Lower Hauterivian	*E. regale*	18.0	0.63	0.06	24.9
Lower Hauterivian	*E. regale*	14.0	0.65	0.04	25.8
Lower Hauterivian	*E. noricum*	9.6	0.63	0.04	24.9
Lower Hauterivian	*E. noricum*	7.5	0.62	0.03	24.4

Speeton section

Substage	Ammonite zone	m above base	TEX86	BIT	T [°C] SST
Upper Hauterivian	*S. gottschei*	37.0	0.59	-	22.9
Upper Hauterivian	*S. gottschei*	32.8	0.57	0.07	21.9
Upper Hauterivian	*S. speetonensis*	23.7	0.60	0.03	23.4
Upper Hauterivian	*S. speetonensis*	18.0	0.62	0.04	24.4

References

Bottini, C., and Mutterlose, J., 2012, Integrated stratigraphy of Early Aptian black shales in the Boreal Realm: calcareous nannofossil and stable isotope evidence for global and regional processes: Newsletters On Stratigraphy, v. 45, p. 115–137.

Geisen, M., Bollmann, J., Herrle, J., Mutterlose, J. and Young, J., 1999, Calibration of the random settling technique for calculation of absolute abundances of calcareous nannoplankton: Micropaleontology, v. 45, p. 437–442.

Heldt, M., Mutterlose, J., Berner, U. and Erbacher, J., 2012, First high-resolution ($\delta^{13}C$ -records across black shales of the Early Aptian Oceanic Anoxic Event 1a within the mid-latitudes of northwest Europe (Germany, Lower Saxony Basin): Newsletters on Stratigraphy, v. 45, p. 151-169.

Kim, J.-H., van der Meer, J., Schouten, S., Helmke, P., Willmott, V., Sangiorgi, F., Koc, N., Hopmans, E.C., and Sinninghe Damsté, J.S., 2010, New indices and calibrations derived from the distribution of crenarchaeal isoprenoid tetraether lipids: Implications for past sea surface temperature reconstructions: Geochimica et Cosmochimica Acta, v. 74, p. 4639–4654, doi:10.1016/j.gca.2010.05.027.

Lehmann, J., Friedrich, O., von Bargen, D. and Hemker, T., 2012, Early Aptian bay deposits at the southern margin of the Lower Saxony Basin: Integrated stratigraphy, palaeoenvironment and OAE 1a: Acta Geologica Polonica v. 62, p. 35−62.

Mutterlose, J., Malkoç, M., Schouten, S., and Sinninghe Damsté, J.S., 2012, Reconstruction of vertical temperature gradients in past oceans –Proxy data from the Hauterivian–early Barremian (Early Cretaceous) of the Boreal Realm: Palaeogeography, Palaeoclimatology, Palaeoecology, v. 363–364, p. 135–143, doi:10.1016/j.palaeo.2012.09.006.

Pauly, S., Mutterlose, J. and Wray, D.S., 2013, Palaeoceanography of Lower Cretaceous (Barremian-Lower Aptian) black shales from northwest Germany evidenced by calcareous nannofossils and geochemistry: Cretaceous Research, v. 42, p. 28−43, doi: 10.1016/j.cretres.2013.01.001.

Smith, A.G., Smith, D.G., Funnell, B.M., 1996, Atlas of Mesozoic and Cenozoic coastlines. Cambridge University Press, Cambridge.

Tiraboschi, D., Erba, E., Jenkyns, H.J., 2009, Origin of rhythmic Albian black shales (Piobbico core, central Italy) Calcareous nannofossil quantitative and statistical analysis and paleoceanographic reconstructions: Paleoceanography, v. 24, p. 2222doi:10.1029/2008PA001670, 2009.